INORGANIC CHEMISTRY

DOI 10.31489/2020Ch4/104-118

UDC 541.128.13

A.K. Zhumabekova[1], L.K. Tastanova[2*], R.O. Orynbassar[3], G.D. Zakumbaeva[4]

[1]*M. Kozybayev North Kazakhstan State University, Petropavlovsk, Kazakhstan;*
[2]*K. Zhubanov Aktobe Regional State University, Aktobe, Kazakhstan;*
[3]*Al-Farabi Kazakh National University, Almaty, Kazakhstan*
[4]*D.V. Sokolskii Institute of Fuel, Catalysis and Electrochemistry, Almaty, Kazakhstan*
(Corresponding author's e-mail: lyazzatt@mail.ru)

Effect of modifiers on Fe-Pt/Al_2O_3 catalysts for alkanes hydrotreatment

Zeolite-containing polyfunctional catalysts Fe-Pt/Al_2O_3 (KT-17, KT-18), modified with additives of molybdenum, phosphorus and cerium, were synthesized. The developed catalytic systems were studied in treatment of C14 alkane obtaining a gasoline fraction. Reaction products contain C4-C9 iso-alkanes, C10-C14 iso-alkanes, C4-C10 alkanes, aromatic hydrocarbons and C1-C3 alkanes. In addition, 0.2–0.6 % of heavy hydrocarbons was found in reaction products. The yield of C4-C9 iso-alkanes at 380 °C reached 37.9 %. By means of physical and chemical methods it has been found that the zeolite containing catalysts Fe-Pt /Al_2O_3 modified by various additives are complex systems. Micro-diffraction and Mossbauer spectroscopy methods allowed detecting nanosized hetero clusters of Fe-Pt, Fe-Mo, Pt-Mo in catalysts structure. Depending on chemical composition of clusters, particle size varies between 20 and 80 Å. KT-18 catalyst demonstrates high activity in the process of heavy alkanes treatment; sizes of platinum (d = 200 Å) and iron (d = 30–50 Å) particles were determined by electron microscopy. Activity of KT-18 catalyst is higher than that of highly dispersed KT-17. The main feature of KT catalysts is their polyfunctionality. During alkanes processing simultaneous and consecutive reactions of hydrocracking, dehydrogenation, isomerization, dehydro-cyclization and hydro-desulfurization take place.

Keywords: hydro treatment, zeolite containing catalysts, modification, polyfunctionality, heavy alkanes, hydrocracking, hydrogenation, nanoclusters.

Introduction

The global trend in oil processing industry development is enhancing the depth of raw materials refining and to improve the quality and environmental characteristics of motor fuels through the use of catalytic systems, which allows obtaining valuable light fractions from heavy oil residues [1, 2].

Production of gasoline fractions from heavy oil is realized in several directions: thermal and catalytic cracking, hydrocracking [3, 4]. Currently, importance of hydrocracking process in oil treatment is relatively low [5]. Thermal and catalytic cracking of heavy oil is widely used in industry [6–9]. However, heavy oil cracking is characterized by obtaining great amount of olefins as a result of C-H bond breakdown [10].

According to the international regulations, content of olefins in gasoline must not exceed 15–18 % [11, 12]. In future, limitations of olefins and aromatic hydrocarbons content in gasoline, in particular benzene concentrations, will become even stricter [13]. Olefins, aromatic hydrocarbons, isoalkanes and oxygen-containing compounds in the form of methyl tert-butyl ether are octane components of gasoline. In this regard, catalytic methods of heavy alkanes hydro isomerization and hydrocracking are widely discussed in literature in recent years [14–18]. Catalysts based on various 3d metals (Ni, Mo, Co, W, Fe, etc.) are used in heavy oil feedstock treatment processes [19–22].

*Corresponding author.

Platinum-based zeolite containing catalysts [17, 23–25], which allow to rise light fraction yields are mainly used in heavy oil hydro treatment.

The aim of the present work is to develop zeolite containing modified polyfunctional catalysts for heavy paraffins hydro processing and to study their properties and performance in tetradecane treatment process.

Experimental

Modified with additives of molybdenum, phosphorus and cerium zeolite-containing polyfunctional catalysts Fe(5 %)-Pt(0,4 %)/Al_2O_3 (KT-17, KT-18) were synthesized. KT-17 contains Mo, P and Ce as modifying additives. KT-18 is modified with cerium and phosphorus.

Properties of catalysts were studied by methods of Electron Microscopy, X-ray phase analysis, BET, IRS, Mossbauer spectroscopy. Genesis of catalyst was studied by Mossbauer spectroscopy method under varying conditions (t, air, H_2). Isomeric shifts (IS) were performed according to α-Fe.

Structure and dimensionality of metal particles, which are the active phase of catalysts, were tested in catalytic transformation of C_{14} alkanes obtaining gasoline fraction. Study was carried out in a stainless steel tubular reactor uniformly coated with electric heater. The reactor was filled first with 3 ml of quartz, then with catalyst (10 ml, d = 2–2.5 mm), pre-treated by hydrogen at 400 °C for 2 hours, and with 3 ml of quartz (particle size is 2–3 mm).

Catalysts were studied in C_{14} treatment process at 280–400 °C temperature range, hydrogen pressure of 2 MPa, H_2:raw material ratio 200:1, and the volume rate of 5 h^{-1}.

0.83 ml / min of raw material was pumped to the reactor by drain pump. The reaction products were cooled and separated, liquid products were collected in the tank, and gas products were directed to gas meter.

The hydrocarbon content of reaction products was analyzed in γ-aluminum oxide stainless steel column of Chrom-4 chromatograph (Supelco) with argon as carrier gas.

Results and Discussion

Specific surface area of synthesized catalysts, measured by the BET method, is 192.5 m^2/g for KT-17 and 222.7 m^2/g for KT-18; porosity is 0.49 cm^3/g and 0.48 cm^3/g respectively (Fig. 1).

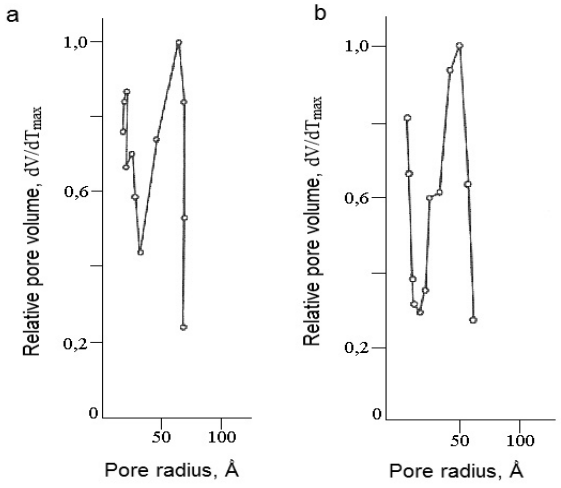

a — KT-17; *b* — KT-18

Figure 1. Porosity of catalytic systems

The KT-17 sample contains two types of narrow and one type of wide pores (Fig. 1, *a*). Narrow pores are available for formation of light hydrocarbons. Wide pores improve the adsorption capacity of catalyst in relation to hydrocarbons processing.

KT-18 catalyst has one type of narrow and wide pores available for adsorption and desorption of hydrocarbons (Fig. 1, *b*). Adsorption and activation of hydrogen and formation of lower alkanes molecules as result of deep hydrocracking of feedstock can occur in narrow pores.

Results of X-ray phase analysis show that catalyst KT-17 has structural elements of HZSM (reflexes 11.4; 6.7; 3.9 Å), Mo (reflex 2.30Å) (ASTM 4–809) and γ-Al_2O_3 (reflex 1.98 Å). Structural elements of HZSM (reflexes 3.84; 3.73 Å) and Al_2O_3 (reflexes 2.26; 1.97; 1.40 Å) were found in catalyst KT-18.

By method of electron microscopy (magnification of 120000) the extensive accumulation of loose particles with size of 80–100 Å was found in catalyst KT-17, micro-diffraction of them shows the formation of phase — Pt_3Mo (ICPDS, 17–719) (Fig. 2, *a*). Small unit of dense particles with size of 50–60 Å is observed in the same catalytic system (Fig. 2, *b*). According to micro-diffraction data, particles have close sets of interplanar distances corresponding to several phases of Pt-Fe: PtFe — tetraferroplatinum (JCPDS, 26–1139); (Pt, Fe) — platinum, ferroan (JCPDS, 29–717, 29–718); Pt_3Fe — isoferroplatinum (JCPDS, 29–716).

Accumulations of large Pt crystals (200 Å) with signs of cutting on the smooth surface of zeolite component of carrier are detected in KT-18 (Fig. 2, *c*). Small rounded clusters (dark particles) composed of CeO_2 particles of 30 Å size are visible. Circular micro-diffraction data of particles with size of 30 Å can be equally attributed to Ce_6O_{11} (JCPDS, 32–196) and Є-Fe_2O_3 (JCPDS, 16–835). Large cluster of 30–50 Å particles, which give circular diffraction of CeO_2 (JCPDS, 34–394) and unit of dense particles of 100–200 Å, microdefraction picture of which is represented by reflexes and can be attributed to sulfur (JCPDS, 27–101), were found in KT-18 (Fig. 2, *d*).

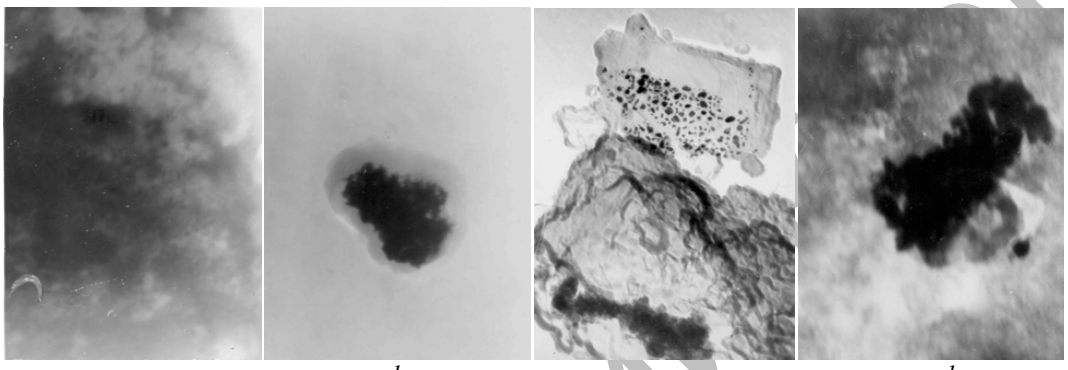

a *b* *c* *d*

a, b — KT-17; *c, d* — KT-18. Magnification 120000

Figure 2. Electron microscopy images of catalytic systems

Table 1 summarizes data on metal active sites of KT-17 and KT-18 catalysts nature.

Table 1

State and structure of particles in calcined (500°C, 5 h) zeolite-containing Pt(0,4 %)-Fe(5 %)/Al_2O_3 catalysts modified with cerium, molybdenum and phosphorus (KT-17) and with cerium and phosphorus (KT-18)

Chemical composition and dispersion of KT-17			
Iron	Platinum	Cerium	Molybdenum
Fe (d = 50–60 Å) $FeFe_2O_4$ (d = 100–300 Å) Fe_2PO_5 (d = 40–80 Å)	Pt (d = 50–60 Å) PtFe (d = 50–60 Å) Pt_3Fe (d = 50–60 Å) Pt_3Mo_2, β-Pt_3Mo (d = 80–100 Å)	CeP_2 (d = 40–50 Å) CeP (d = ~300 Å)	$MoOPO_4$ (d = ~15 Å) MoO_2 (d = 100–300 Å)
Chemical composition and dispersion of KT-18			
Iron	Platinum	Cerium	
Є-Fe_2O_3 (30 Å) η-Fe_2O_3 (d = 30–50 Å) Fe_2O_3 (d = 30–50 Å)	Pt (d = 200 Å)	CeO_2 (d = 30–50 Å) CeP (d = 100–200 Å) Ce_6O_{11} (d = 30 Å) $CeAlO_3$ (d = 30–50 Å)	

As it can be observed from Table 1, KT-17 catalyst sample contains homonuclear particles of Pt and Fe (50–60 Å), Fe_2PO_5, $MoOPO_4$ (15–300 Å) compounds, as well as homonuclear and heteronuclear clusters. Homonuclear clusters include $FeFe_2O_4$, molybdenum oxide MoO_2, the size of which varies from 100 to 300 Å. Heteronuclear clusters include PtFe, Pt_3Fe, Pt_3Mo_2, β-Pt_3Mo, CeP_2, CeP. These heteronuclear clusters have dimensions from 40 to 100 Å and 300 Å. According to electron-microscopic studies, KT-17 catalyst is nanostructured system of complex composition with particle sizes mainly from 15 to 100 Å.

KT-18 catalyst sample contains homonuclear particles of Pt, 200 Å in size, iron oxides and cerium oxides, the sizes of which range from 30 to 50 Å (Table 1). Heteronuclear cluster CeP (100–200 Å) and

$CeAlO_3$ compound (30–50 Å) were also found in this catalyst. The detected structures have different dimensions, mainly from 30 to 200 Å.

Catalysts were studied with Mossbauer spectroscopy method at varying conditions (t, Ar, H_2, O_2).

Spectra of initial systems (KT-17, KT-18) are superpositions of two doublets corresponding to high-spin states of Fe_1^{3+} and Fe_2^{3+} with similar values of isomeric shifts (0.30–0.31 mm/s), which are distinguished by quadruple splitting (QS): Fe_1^{3+} — 1,59 mm/s and Fe_2^{3+} — 0,95 mm/s. Fe_1^{3+}/Fe_2^{3+} ratio is ~ 2/3. Since the line width corresponding to these structures is large (0.64 mm/s), it can be assumed that the forms of Fe^{3+} represent a set of close states with approximately the same isomeric shift (IS) and different quadruple splittings due to differences in the environment of iron.

The form with higher QS in KT-17 can be attributed to iron ions located on the surface of matrix. Values of isomeric shift raise with temperature growth, while the quadruple splitting practically does not change (Table 2).

Table 2

Mossbauer parameters and relative amount (S, %) of different forms of iron in KT-17 catalyst in air

Temperature, °C	Fe_1^{3+}			Fe_2^{3+}		
	IS, mm/s	QS, mm/s	S, %	IS, mm/s	QS, mm/s	S, %
20	0.31	1.43	42	0.31	0.84	58
100	0.27	1.40	42	0.27	0.85	58
200	0.21	1.39	43	0.20	0.86	57
300	0.14	1.43	42	0.14	0.85	58
400	0.07	1.45	41	0.07	0.89	59
500	0.02	1.39	45	0.00	0.94	55

Reduction of iron in catalytic system KT-17 starts in hydrogen stream at 100 °C, forming up to 3 % of Fe^{2+} (Fig. 3). At 200 °C, ~ 27 % of Fe^{2+} in two states, corresponding to two initial states of Fe^{3+}, is present in system. The Fe_1^{2+} form with high QS is located on the surface as well as Fe_1^{3+}. At 400 °C, one form of Fe^{3+} is more deeply located in the carrier, and two forms of Fe^{2+} remain in the system. At 500 °C, system contains only two forms of Fe^{2+}.

Temperature decline from 500 to 100 °C (reverse) does not lead to new forms of iron (Table 3). However, redistribution of intensities of Fe^{2+} relative content signals takes place: the intensity of signal of iron form with higher QS increases, due to this effect's dependence on temperature. This is explained by weak interaction of Fe_1^{2+} form with carrier, since it is located on the surface. One more form of iron with Mossbauer parameters which are characteristic for Fe-Pt clusters located on the surface appears in system at 20 °C (Table 3).

Table 3

Mossbauer parameters and relative amount (S, %) of different forms of iron in KT-17 catalyst at varying temperature in hydrogen atmosphere

t, °C	Fe_1^{3+}			Fe_2^{3+}			Fe_1^{2+}			Fe_2^{2+}			Fe-Pt phase		
	IS, mm/s	QS, mm/s	S, %	IS, mm/s	QS, mm/s	S, %	IS, mm/s	QS, mm/s	S, %	IS, mm/s	QS, mm/s	S, %	IS, mm/s	QS, mm/s	S, %
20	0.31	1.53	37	0.30	0.92	63									
100	0.25	1.45	45	0.27	0.87	52	1.22	2.78	3						
200[1]	0.21	1.42	37	0.20	0.85	37	0.94	1.99	15	0.86	1.32	11			
300	0.14	1.43	8	0.14	0.85	14	0.86	1.87	45	0.81	1.14	33			
400[2]				0.12	1.03	11	0.82	1.66	47	0.72	1.10	42			
500							0.75	1.55	41	0.65	1.09	59			
400							0.80	1.70	51	0.71	1.07	49			
300							0.88	1.73	63	0.75	1.19	37			
200							0.94	1.95	64	0.85	1.21	36			
100							1.02	2.11	69	0.90	1.34	31			
20							1.08	2.21	59	1.00	1.39	25	0.33	1.13	16

Notes: [1] — Fe^{2+} forms were not distinguished due to their small amounts at 200°C; [2] — Fe^{3+} forms were not distinguished due to their small amounts at 400 °C.

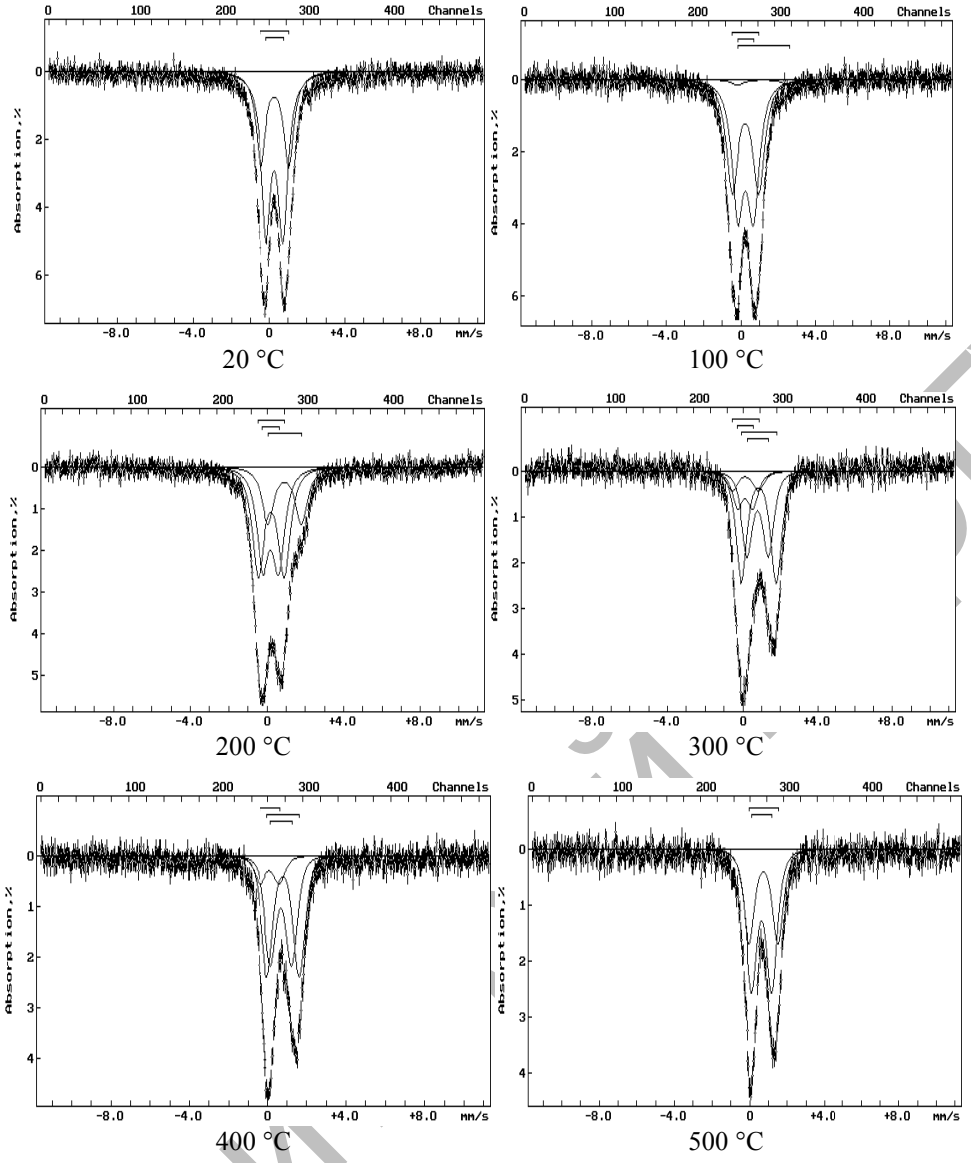

Figure 3. Mossbauer spectra of KT-17 catalytic system at varying temperature. Atmosphere — hydrogen

In air stream at 20 °C after reduction by hydrogen system contains two forms of Fe^{3+} and two forms of Fe^{2+}, Fe-Pt phase disappears (Fig. 4, *a*). More high QS value for Fe^{3+} forms than it was observed before the start of reduction cycle draws attention (Table 4). Replacing of air with hydrogen at the same temperature leads to a noticeable growth of Fe^{2+} forms amounts (Fig. 4, *b*).

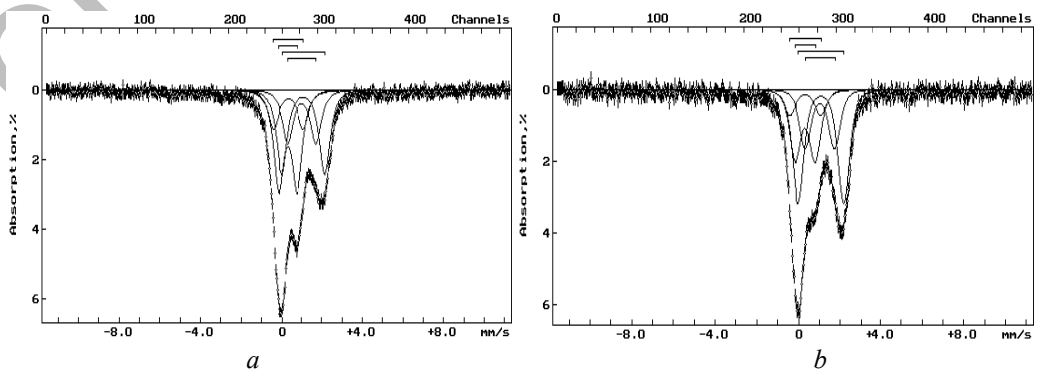

Figure 4. Mossbauer spectra of KT-17 catalytic system at 20 °C obtained after reduction and cooling in the atmosphere of: a) air, b) hydrogen

Obtained at 20 °C spectrum of system calcined at 500 °C in air is a superposition of two doublets corresponding to two states of Fe^{3+}, just as it was observed for the initial state of system (Fig. 5, *a*. Table 4). However, even in this case, the observed values of quadruple splitting are much higher.

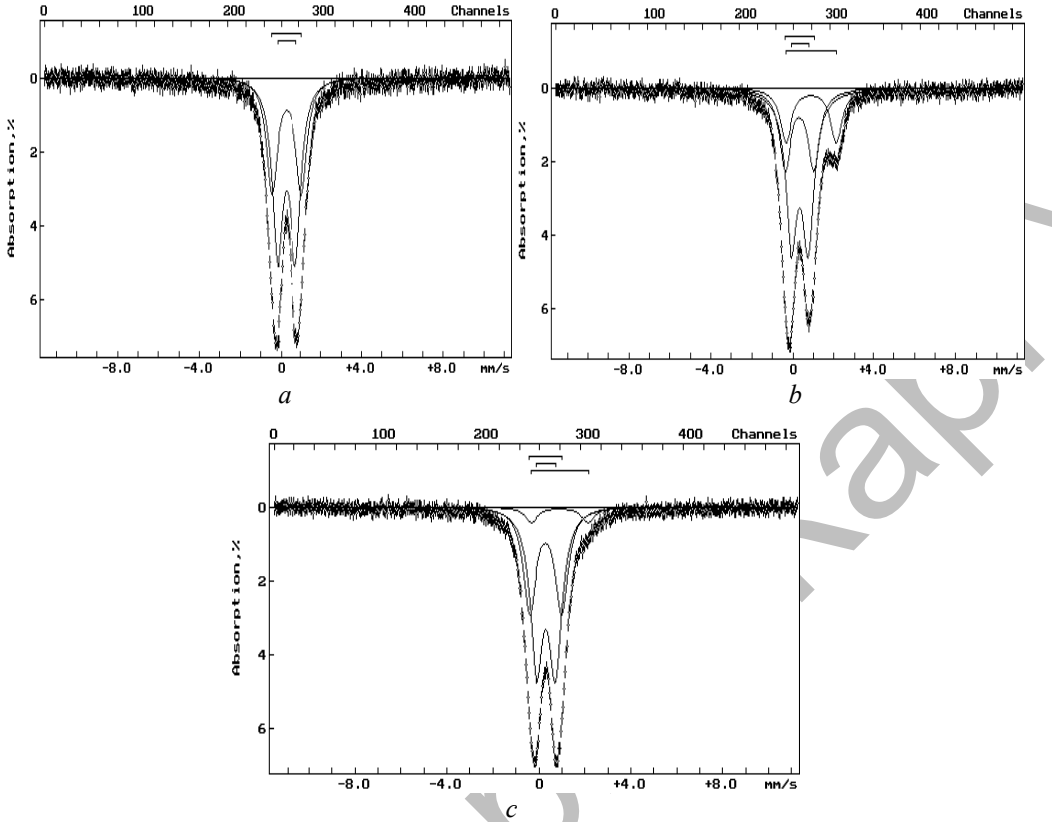

Atmosphere: *a* — air; *b* — hydrogen; *c* — air (after hydrogen)

Figure 5. Mossbauer spectra of KT-17 catalytic system at 20 °C obtained after oxidation at 500 °C

Table 4

Mossbauer parameters and relative amount (S, %) of different forms of iron in KT-17 at 20 °C

Fe_1^{3+}			Fe_2^{3+}			Fe_1^{2+}			Fe_2^{2+}			Fe-Pt phase		
IS, mm/s	QS, mm/s	S, %	IS, mm/s	QS, mm/s	S, %	IS, mm/s	QS, mm/s	S, %	IS, mm/s	QS, mm/s	S, %	IS, mm/s	QS, mm/s	S, %
In air stream after reduction by H_2														
0.34	1.52	14	0.32	0.95	36	1.09	2.17	31	1.03	1.43	19			
In H_2 after air														
0.33	1.51	10	0.33	0.97	26	1.09	2.20	42	1.04	1.41	22			
In air (after heating in air at 500 °C)														
0.30	1.53	40	0.30	0.94	60									
In H_2 after calcination at 500 °C in air and cooling														
0,33	1.43	28	0.35	0.83	53							0.89	2.48	19
In air after reduction by H^2 at 20 °C														
0,30	1.43	38	0.32	0.84	57							0.91	2.48	5

After calcination at 500 °C in air and cooling, hydrogen was supplied to the system at 20 °C. In this case, partial reduction occurred and, in addition to the forms of Fe^{3+}, ~ 19 % of Fe^{2+} appeared in system, however, the Mossbauer parameters of this form differed from the previously observed parameters of Fe^{2+} forms (Fig. 5, *b*. Table 4). In papers [26, 27] such behavior of systems, i.e. the ability to reduce at room temperature was considered indisputable evidence of the presence of Fe-Pt, Fe-Pd, Fe-Rh clusters. It is noteworthy that there is a very good quantitative correspondence between relative content of Fe-Pt phase at 20 °C

after fall of temperature from 500 °C in hydrogen atmosphere (Table 4) and its relative content after reduction at room temperature of system calcined in air at 500 °C (Table 3) — 19 % and 16 %, respectively.

After replacing of hydrogen by air at 20 °C, partial oxidation of Fe-Pt phase takes place, its relative content is reduced to ~ 5 % (Fig. 5, *c*. Table 4).

When calcined in air, the isomeric shift in catalytic system KT-18 decreases, and quadruple splitting raises from 1.59 to 1.70–1.74 mm/s (Fig. 6, *a*). Replacing air with hydrogen at 100 °C leads to appearance of two forms of Fe^{2+} (18 %), which are formed when the initial states of $Fe^{3+}$are reduced (Fig. 6, *b*). With repeated redox treatment (20–500 °C), concentration of Fe^{2+} forms increases from 18 to 60 % (t = 200 °C) (Fig. 6, *c*).

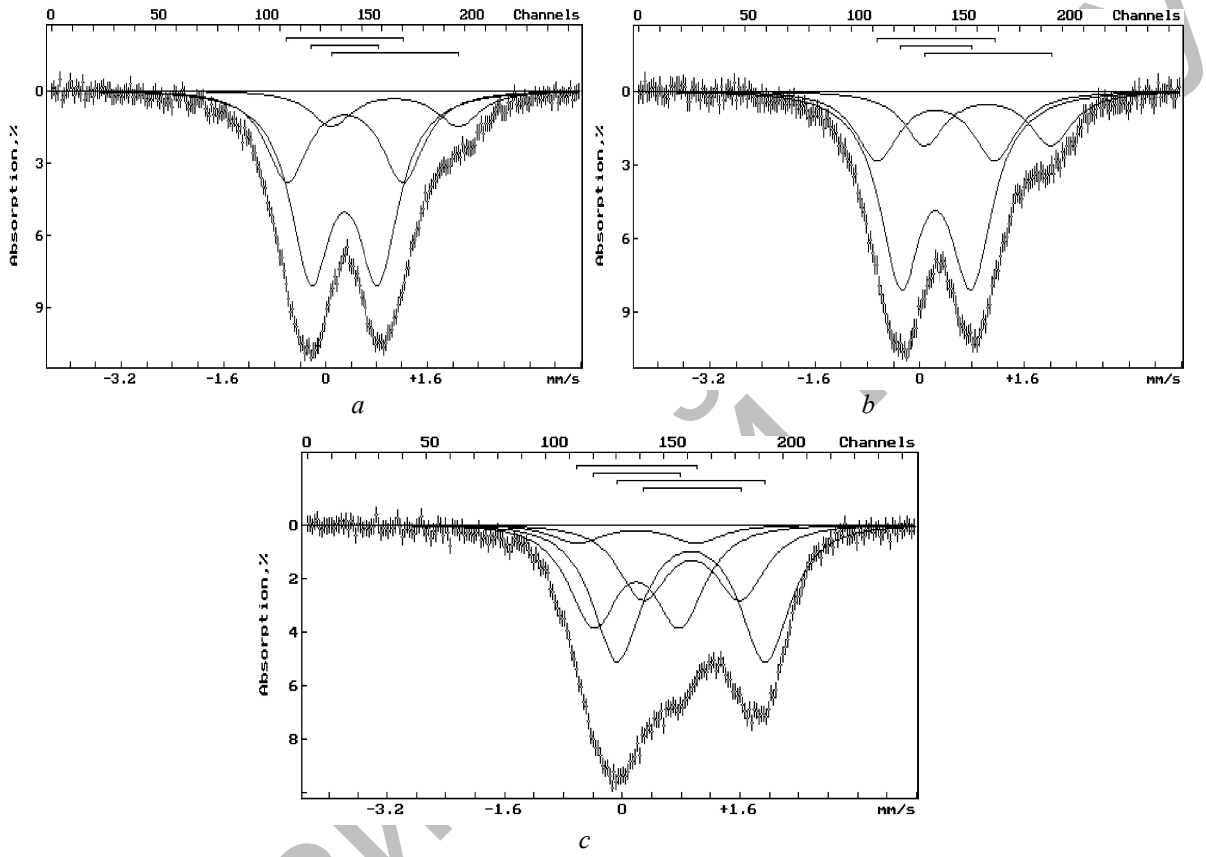

a — 20 °C — air, after oxidation at 500 °C; *b* — 100 °C — hydrogen, after oxidation at 500 °C; *c* — reduction with hydrogen at 200 °C, after oxidation at 500 °C

Figure 6. Mossbauer spectra of KT-18 catalytic system at varying temperature

According to IR spectra of ammonia adsorption (10 min) on KT-17 catalyst at room temperature, the adsorption bands are fixed at 3370, 3320, 3250, 1620, 1580 and 1450 cm^{-1} (Fig. 7, spectrum 1). The absorption bands at 3370, 3320, 1620 cm^{-1} belong to Lewis acid centers, and at 3250, 1580, 1450 cm^{-1} characterize Bronsted acid centers. After evacuation of sample, absorption bands are found at 1620, 1420 cm^{-1} (Fig. 7, spectrum 2).

During ammonia adsorption at 250 °C (for 10 min), adsorption bands are detected at 3370, 3300, 1710, 1600 and 1420 cm^{-1} (Fig. 7, spectrum 3). The absorption bands at 3370, 3300, 1600 cm^{-1} are due to formation of coordination bond of ammonia at Lewis centers of zeolite. Surface reaction of ammonia with the Bronsted center forming NH_4^+ gives absorption bands at 1710 and 1420 cm^{-1}. After the sample has been evacuated, absorption bands are present at 3230, 1620 and 1440 cm^{-1} (Fig. 7, spectrum 4).

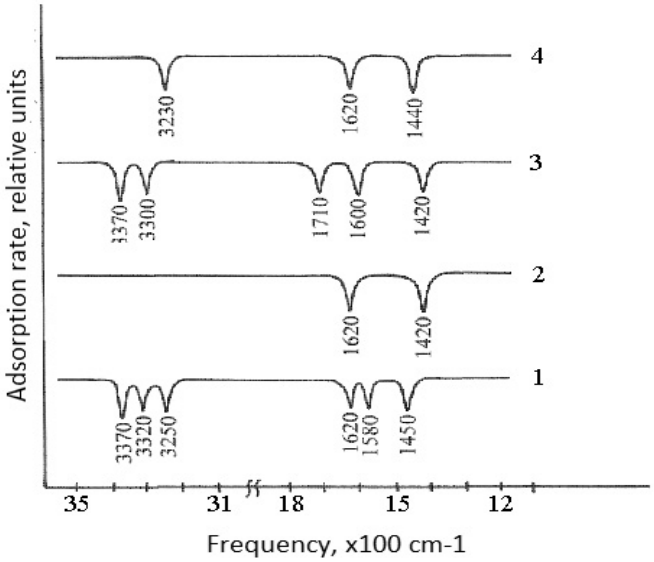

1 — NH_3 adsorption at room temperature; *2* — evacuation; *3* — NH_3 adsorption at t = 250 °C; *4* — evacuation

Figure 7. IR spectra of NH_3 adsorption on KT-17 catalyst

On IR spectrum of ammonia adsorbed on KT-18 catalyst at room temperature (for 15 min), adsorption bands are fixed at 3420, 3350, 3270, 3200, 1720, 1620, 1500 and 1410 cm^{-1} (Fig. 8, spectrum 1). Adsorption bands at 3420, 3350 and 1620 cm^{-1} characterize Lewis acid centers, and adsorption bands at 3270, 3200, 1720, 1500 and 1410 cm^{-1} refer to Bronsted acid centers. After the sample was evacuated, the adsorption bands were found at 1600 and 1450 cm^{-1} (Fig. 8, spectrum 2), they belong to the most active of Lewis and Bronsted acid centers.

During the adsorption of ammonia on catalyst for 15 min at 250 °C, the adsorption bands were found at 3550, 3450, 3300, 3160, 1620, 1560 and 1460 cm^{-1}, which characterize the ammonia molecule coordination bounded with the Lewis centers (3450, 3300, 1620 cm^{-1}), and indicate formation of ammonium ions — surface reaction with the Bronsted centers (3550, 3160, 1560, 1460 cm^{-1}) (Fig. 8, spectrum 3). After evacuation, adsorption bands are observed at 1600, 1450 cm^{-1} (Fig. 8, spectrum 4).

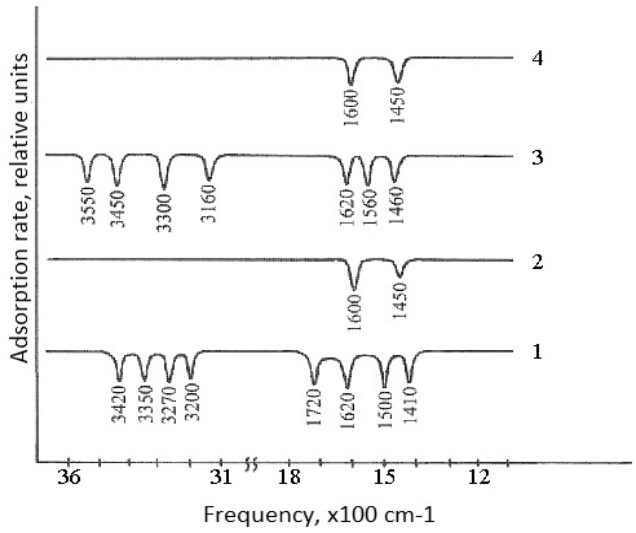

1 — NH_3 adsorption at room temperature; *2* — evacuation;
3 — NH_3 adsorption at t = 250 °C; *4* — evacuation

Figure 8. IR spectra of NH_3 adsorption on KT-18 catalyst

Process of tetradecane hydro treatment on KT-17 and KT-18 catalysts was studied. Conversion of tetradecane on KT-17 grows from 59.1 to 94.8 % with rising temperature (Table 5). Reaction products contain C_4-C_9 iso-alkanes, C_{10}-C_{14} iso-alkanes, C_4-C_{10} alkanes, aromatic hydrocarbons and C_1-C_3-alkanes. In addition, 0.2–0.6 % of C_{14+} heavy hydrocarbons is found in reaction products. The yield of C_4-C_9 iso-alkanes at 380 °C reaches 37.9 %. It is known that gasoline fraction contains isoalkanes, n-alkanes, aromatic hydrocarbons and olefins. When tetradecane is transformed, hydrocracking of tetradecane proceeds with formation of mainly iso- and n-alkanes, content of aromatic hydrocarbons varies from 3.3 to 0.7 %.

The presence of C_4-C_9 normal and iso-alkanes, aromatic hydrocarbons, C_1-C_3 alkanes and C_{14+} hydrocarbons in reaction products demonstrates that KT-17 catalyst provides the parallel flow of hydrocracking, hydro-isomerization, dehydro-cyclization and alkylation reactions, thus proving its polyfunctional properties. According to the content of reaction products, tetradecane is almost totally converted. Yield of gasoline fraction is 67.9 % at 380 °C.

Table 5

Tetradecane hydro treatment over KT-17 and KT-18 catalysts. P = 2MPa, V = 5 h^{-1}, H_2:raw materials = 200:1

Products content, %	Temperature of the process, °C					
	280	300	320	350	380	400
KT-17						
Conversion	59.1	68.6	71.5	75.0	91.4	94.8
∑ C_4-C_9 iso-alkanes	35.3	31.3	33.4	32.4	37.9	36.2
∑ C_{10}-C_{14} iso-alkanes	3.3	2.2	1.9	1.6	1	1.1
∑C_1-C_3	1.4	10.4	12.0	15.5	22.1	27.3
∑ C_4-C_9 normal chain alkanes	15.2	21.1	20.5	23.4	28.3	29.3
∑ aromatic hydrocarbons	3.3	3.2	3.3	1.8	1.7	0.7
C_{14+}	0.6	0.4	0.4	0.3	0.1	0.2
Initial tetradecane	40.9	31.4	28.5	25.0	8.6	5.2
Yield of gasoline fraction	53.8	55.6	57.2	57.6	67.9	66.2
KT-18						
Conversion	64,9	94.4	98.7	99.4	99.7	100
∑ C_4-C_9 iso-alkanes	33.2	44.4	42.4	42.6	36.1	33.0
∑ C_{10}-C_{14} iso-alkanes	4.8	5.6	2.8	1.9	1.0	2.3
∑C_1-C_3	4.9	9.5	12.9	22.6	27.8	28.2
∑ C_4-C_9 normal chain alkanes	18.9	27.3	35.2	28.4	32.5	33.2
∑ aromatic hydrocarbons	3.1	6.8	5.0	3.7	2.2	2.8
Olefins	-	0.8	0.4	0.2	0.1	0.5
Initial tetradecane	35.1	5.6	1.3	0.6	0.3	traces
Yield of gasoline fraction	55.2	79.3	83.0	74.9	70.9	69.5

Conversion of tetradecane on KT-18 raises from 64.9 to 100 % with temperature growth from 280 to 400 °C. Reaction products contain C_4-C_9 n-alkanes, C_4-C_9 and C_{10}-C_{14} iso-alkanes, aromatic compounds (benzene, toluene, o- and p-xylenes) and olefins. Light C_1-C_3-hydrocarbons are presented with ethane, propane, ethylene and propylene; their yield rises from 4.9 to 28.2 % as temperature grows. The presence of the above mentioned organic compounds in reaction products indicates parallel sequential course of hydrocracking, dehydrogenation, isomerization, and alkylation reactions.

In liquid products content of isoalkanes C_4-C_9 prevails in the whole temperature range, the maximum yield of which (44.4 %) is observed at 300 °C. Formation of heavy isoalkanes C_{10}-C_{14} under these conditions does not exceed 5.6 %. Quantity of C_4-C_9 n-alkanes and aromatic compounds is equal to 35.2 % (t = 320 °C) and 6.8 % (t = 300 °C) respectively. At temperature growth above 300 °C yield of liquid products reduces and deep hydrocracking of tetradecane to C_1-C_3 hydrocarbons increases; concentration of these hydrocarbons at 400 °C rises to 28.2 % (Table 5). Yield of gasoline fractions is maximal at 320 °C (83.0 %).

The temperature dependence of tetradecane conversion and isoalkanes C_4-C_9 output on KT group catalysts is presented in Figure 9.

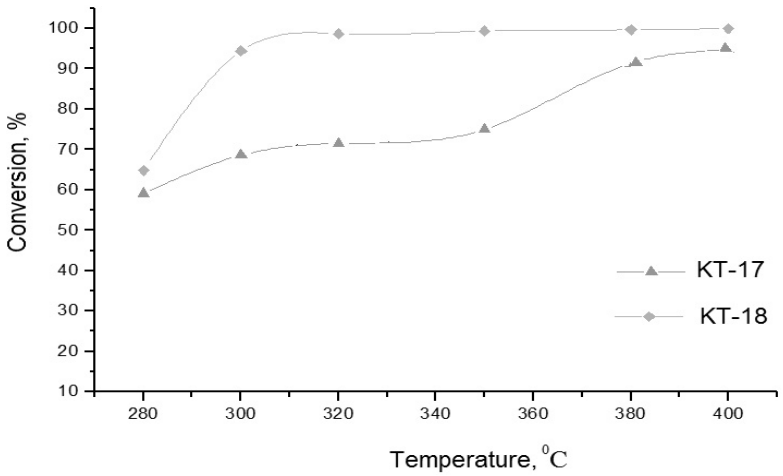

P_{H_2} = 2 MPa; V_v = 5 h^{-1}, H_2:raw materials = 200:1

Figure 9. Influence of temperature on tetradecane conversion on zeolite-containing Pt-Fe/Al_2O_3 catalysts

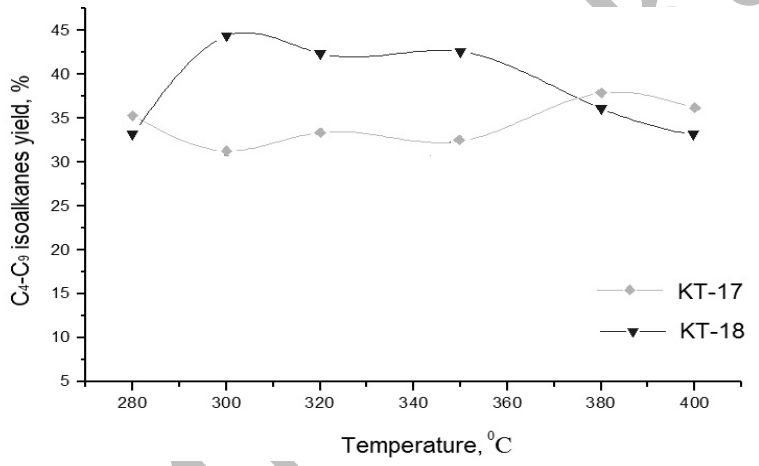

P_{H_2} = 2 MPa; V_v = 5 h^{-1}, H_2:raw materials = 200:1

Figure 10. Influence of temperature on the output of isoalkanes C_4-C_9 at tetradecane transformation on zeolite-containing Pt-Fe/Al_2O_3 catalysts

It is clear (Fig. 9 and 10) that KT-18 catalyst is more optimal in the whole temperature range. This is probably due to a certain dispersion state of platinum (d = 200 Å), as the adsorption and activation of high molecular weight alkanes require flat orientation at active centers located on smooth surface of zeolite or near the mouths of pores. Cavities with d = 56–53 Å, typical for ZSM-5 zeolite, are inaccessible for heavy alkane molecules. Electron microscopy method shows that part of platinum in KT-18 catalyst is localized on the surface of zeolite (Fig. 2, *c*). At 300 °C the yield of C_4-C_9 isoalkanes is 44.4 %.

The observed direction of tetradecane transformations can be related to the combination of acid and hydro-dehydrating properties of catalysts, due to localization of platinum and Fe-Pt clusters on crystalline surface and in zeolite channels. It can be assumed that hydrocracking takes place on the active centers of Pt-zeolite, which are formed on the external crystal structure of zeolite. Smaller fragments of surface-activated decomposition particles of heavy n-alkanes can migrate into zeolite channels, where mono- and bimetallic clusters of platinum and Fe-Pt, which take part in waterproofing and hydro-isomerization with formation of isoalkanes C_4-C_9, are localized. The low yield of C_{10}-C_{15} isoalkanes can be explained by competitive hydrocracking reaction on platinum-promoted external crystalline surface of zeolite. Deep hydrocracking of heavy alkanes on active centers of catalyst becomes prevailing at high temperatures. Narrow size of channels (0.56–0.53 nm) of ZSM-5 zeolite complicates diffusion of large molecules of n-alkanes with high molecular weight.

Conclusions

The synthesized catalysts can be referred to nanostructured and nanosized catalytic systems. Size of metal particles in catalysts varies from 20 to 100 Å, at the same time particles with sizes of 150–200 Å and, as an exception, of 300–500 Å were found, in particular for molybdenum.

Along with nanosized homonuclear particles of metals, heteronuclear clusters consisting of two different elements are formed in the studied catalysts. Structure and dimension of Pt-Fe clusters depend on the nature of promoting additives. Two structures of heteronuclear clusters were detected in KT-17 catalyst: Pt-Fe (d = 50–60 Å) and Pt_3Fe (d = 50–60 Å). Along with iron, platinum forms heteronuclear clusters with molybdenum: Pt_3Mo_2, β-Pt_3Mo (d = 80–100 Å).

Composition and structure of catalysts are greatly influenced by cerium, which, as a precursor, is primarily responsible for high resistance of catalyst granules to abrasion, and secondly — cerium, forming various compounds (Ce_6O_{11}, CeP_2, CeP, $CeAlO_3$, Ce_2O_3, CeO_2, $Ce(MoO_4)_2$, $Ce_2Mo_3O_{12}$) prevents diffusion and agglomeration of platinum and iron particles. Metals of group VIII at high temperatures have a certain tendency to sintering and crystallization.

It follows from the analysis of structure and chemical composition of synthesized catalysts that acid zeolite centers, homo- and heteronuclear metal clusters are the active components involved in reaction of tetradecane transformation. It should be noted that acid and metal centers are located close to each other or combined into a single active center. This is confirmed by electron microscopy images.

Scheme of the mechanism of tetradecane transformation:

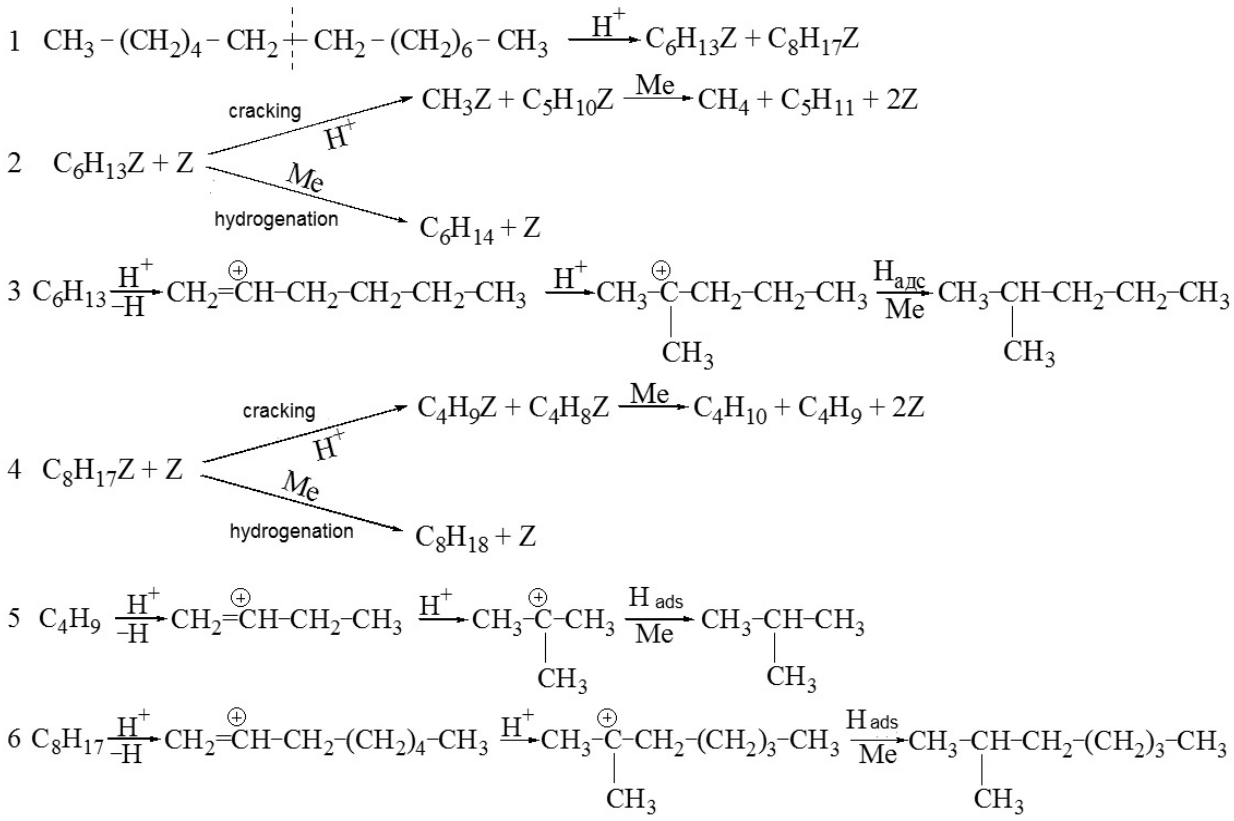

Hydrocracking reactions and dehydrogenation of n-alkanes into semi-hydrated form and olefins take place on the active centers after their recovery by hydrogen. Olefins are transformed on the Bronsted acid centers through carbenium-ion into isoolefins, which form isoalkanes interacting with M-H_{ads} (M — metal).

The proposed mechanism is confirmed by presence of olefins and surface activated complexes preceding the formation of isoolefins in gaseous products C_2-C_4. Due to their transformation into iso-alkanes at subsequent stages, their presence in the final products of reaction is insignificant.

Hydrogenation reactions of both iso-olefins and CH_3- and other alkyl groups to light gaseous hydrocarbons take place with participation of hydrogen on the active centers of catalyst in parallel with isomerization. It is necessary to note formation of aromatic hydrocarbons (benzene, toluene, xylenes) along with the above

described reactions of tetradecant transformation. This reaction occurs mainly in high temperature area (350–400 °C). It is assumed that mononuclear particles of platinum also take part in tetradecane dehydrocyclization and dehydrogenation.

KT-18 catalyst demonstrates high activity in the process of heavy alkanes treatment; sizes of platinum (d = 200 Å) and iron (d = 30–50 Å) particles were determined by electron microscopy. Activity of KT-18 catalyst was higher than that of highly dispersed KT-17, because flat clusters have to be situated near the active sites of catalyst in order to destruct C_4-C_5 and C_9-C_{10} bonds of C_4-C_9 normal and iso-alkanes.

Gasoline fraction with an output from 30.2 to 83.0 % containing 17.7–42.4 % of isoalkanes, 1.7–5.0 % of aromatic hydrocarbons, 0.3–0.4 % of olefins and 10.5–35.2 % of C_4-C_9 n-alkanes was received at tetradecane hydro processing on KT-18.

In general, the process is carried out relatively easily in the presence of large particles of platinum, concentrated on the outer surface or in cavities of zeolite.

Highly dispersed metal phase of HZSM zeolite cavities (53–56 Å) is not subjected to change and adsorption of long-chain alkanes under soft conditions.

The main feature of KT catalysts is their polyfunctionality. During alkanes processing simultaneous and consecutive reactions of hydrocracking, dehydrogenation, isomerization, dehydro-cyclization and hydrodesulfurization take place.

By means of physical and chemical methods it has been found that the zeolite containing catalysts Fe-Pt/Al_2O_3 modified by various additives are complex systems. Micro-diffraction and Mossbauer spectroscopy methods allowed detecting nanosized hetero clusters of Fe-Pt, Fe-Mo, Pt-Mo in catalysts structure. Depending on chemical composition of clusters, particle size varies between 20 and 80 Å. Catalysts are not exposed to carbonization, they are stable and highly active, therefore these systems can be proposed for practical testing.

References

1 Rana M.S. A review of recent advances on process technologies for upgrading of heavy oils and residua / M.S. Rana, V. Sarmano, J. Ancheyta, J.A.I. Diaz // Fuel. — 2007. Vol. 86, No. 9. — P. 1216–1231. DOI: 10.1016/j.fuel.2006.08.004

2 Okunev A.G. Catalytic hydroprocessing of heavy oil feedstocks / A.G. Okunev, E.V. Parkhomchuk, A.I. Lysikov, P.D. Parunin, V.S. Semeykina, V.N. Parmon // Russian Chemical Reviews. — 2015. — Vol. 84, No. 9. — P. 981–999. DOI: 10.1070/RCR4486

3 Sahu R. A review of recent advances in catalytic hydrocracking of heavy residues / R. Sahu, B.J. Song, J.S. Im, Y-P. Jeon, C.W. Lee // Journal of Industrial and Engineering Chemistry. — 2015. — Vol. 27. — P. 12–24. DOI: 10.1016/j.jiec.2015.01.011

4 Fujimoto K. Hydrothermal cracking of residual oil / K. Fujimoto, J. Chang, N. Tsubaki // Sekiyu Gakkaishi — Journal of the Japan Petroleum Institute. — 2000. — Vol. 43, No. 1. — P. 25–36.

5 Gillis D. Upgrading Residues to Maximize Distillate Yields with UOP Uniflex (TM) Process / D. Gillis, M. VanWees, P. Zimmerman, E. Houde // Journal of the Japan Petroleum Institute. — 2010. — Vol. 53, No. 1. — P. 33–41. DOI: 10.1627/jpi.53.33

6 Corma A. Crude oil to chemicals: light olefins from crude oil / A. Corma, E. Corresa, Y. Mathieu, L. Sauvanaud, S. Al-Bogami, M.S. Al-Ghrami, A. Bourane // Catalysis Science & Technology. — 2017. — Vol. 7, No. 1. — P. 12–46. DOI: 10.1039/c6cy01886f

7 Nazarova G.Y. Effect of group composition of the vacuum distillate from heavy Kazakhstan and West Siberian oil on the yield of light fractions during the catalytic cracking / G.Y. Nazarova, E.N. Ivashkina, E.D. Ivanchina, V.I. Stebeneva, G.Z. Seytenova // Procedia Engineering. — 2016. — Vol. 152. — P. 18–24. DOI: 10.1016/j.proeng.2016.07.611

8 Kaminski T. Thermal cracking of atmospheric residue versus vacuum residue / T. Kaminski, M.M. Husein // Fuel Processing Technology. — 2018. — Vol. 181. — P. 331–339. DOI: 10.1016/j.fuproc.2018.10.014

9 Ghashghaee M. Two-Step Thermal Cracking of an Extra-Heavy Fuel Oil: Experimental Evaluation, Characterization, and Kinetics / M. Ghashghaee, S. Shirvani // Industrial and Engineering Chemistry Research. — 2018. — Vol. 57, No. 22. — P. 7421–7430. DOI: 10.1021/acs.iecr.8b00819

10 Vogt E.T.C. Fluid catalytic cracking: recent developments on the grand old lady of zeolite catalysis / E.T.C. Vogt, B.M. Weckhuysen // Chemical Society Reviews. — 2015. — Vol. 44, No. 20. — P. 7342–7370. DOI: 10.1039/c5cs00376h

11 Onoichenko S.N. Current and Promising Automotive Gasolines / S.N. Onoichenko, V.E. Emel'yanov, I.F. Krylov // Chemistry and technology of fuels and oils. — 2003. — Vol. 39, No. 6. — P. 303–308. DOI: 10.1023/B: CAFO.0000011901.59445.22

12 Hajbabaei M. Impact of olefin content on criteria and toxic emissions from modern gasoline vehicles / M. Hajbabaei, G. Karavalakis, J.W. Miller, M. Villela, K.H. Xu, T.D. Durbin // Fuel. — 2013. — Vol. 107. — P. 671–679. DOI: 10.1016/j.fuel.2012.12.031

13 Courty P. Refining Clean Fuels for the Future / P. Courty, J.F. Gruson // Oil & Gas Science and Technology. — 2001. — Vol. 56, No. 5. — P. 515–524. DOI: 10.2516/ogst:2001041

14 Castaneda L.C. Combined process schemes for upgrading of heavy petroleum / L.C. Castaneda, J.A.D. Munoz, J. Ancheyta // Fuel. — 2012. — Vol. 100. — P. 110–127. DOI: 10.1016/j.fuel.2012.02.022

15 Bellussi G. Hydroconversion of heavy residues in slurry reactors: Developments and perspectives / G. Bellussi, G. Rispoli, A. Landoni, R. Millini, D. Molinari, E. Montanari, D. Moscotti, P. Pollesel // Journal of Catalysis. — 2013. — Vol. 308. — P. 189–200. DOI: 10.1016/j.jcat.2013.07.002

16 Zaki T. Slurry-phase catalytic hydrocracking of mazut (heavy residual fuel oil) using Ni-bentonite / T. Zaki, G.S. Mukhtarova, A.M. Al-Sabagh, F.S. Soliman, M.A. Betiha, T. Mahmoud, M. Abd El-Raouf, N.K. Afandiyeva, A. Alizade, A.B. Hasanova, V.M. Abbasov // Petroleum Science and Technology. — 2018. — Vol. 36, No. 19. — P. 1559–1567. DOI: 10.1080/10916466.2018.1490762

17 Martens J.A. Hydroisomerization and hydrocracking of linear and multibranched long model alkanes on hierarchical Pt/ZSM-22 zeolite / J.A. Martens, D. Verboekend, K. Thomas, G. Vanbutsele, J. Perez-Ramirez, J.P. Gilson // Catalysis Today. — 2013. — Vol. 218. — P. 135–142. DOI: 10.1016/j.cattod.2013.03.041

18 Batalha N. n-Hexadecane hydroisomerization over Pt-HBEA catalysts. Quantification and effect of the intimacy between metal and protonic sites / N. Batalha, L. Pinard, C. Bouchy, E. Guillon, M. Guisnet // Journal of Catalysis. — 2013. — Vol. 307. — P. 122–131. DOI: 10.1016/j.jcat.2013.07.014

19 Sosnin G.A. Catalytic steam cracking of vacuum residue in presence of dispersed catalysts based on Mo, Ni, Fe, Co, Al metals / G.A. Sosnin, O.O. Zaikina, P.M. Eletskii, V.A. Yakovlev / Bulletin of the Tomsk Polytechnic University — Geo Assets Engineering. — 2018. — Vol. 329, No. 12. — P. 145–154. DOI: 10.18799/24131830/2018/12/30

20 Mironenko O.O. Catalytic Steam Cracking of Heavy Crude Oil with Molybdenum and Nickel Nanodispersed Catalysts / O.O. Mironenko, G.A. Sosnin, P.M. Eletskii, Y.K. Gulyaeva, O.A. Bulavchenko, O.A. Stonkus, V.O. Rodina, V.A. Yakovlev // Catalysis in Industry. — 2017. — Vol. 9, No. 3. — P. 221–229. DOI: 10.1134/S2070050417030084

21 Alphazan T. Highly active nonpromoted hydrotreating catalysts through the controlled growth of a supported hexagonal WS2 phase / T. Alphazan, A. Bonduelle-Skrzypczak, C. Legens, A.S. Gay, Z. Boudene, M. Girleanu, O. Ersen, C. Coperet, P. Raybaud // ACS Catalysis. — 2014. — Vol. 4, No. 12. — P. 4320–4331. DOI: 10.1021/cs501311m

22 Funai S. Recovery of useful lighter fuels from petroleum residual oil by oxidative cracking with steam using iron oxide catalyst / S. Funai, E. Fumoto, T. Tago, T. Masuda // Chemical Engineering Science. — 2010. — Vol. 65, No. 1. — P. 60–65. DOI: 10.1016/j.ces.2009.03.028

23 Alvarez F. Hydroisomerization and hydrocracking of alkanes — Influence of the balance between acid and hydrogenating functions on the transformation of n-decane on PtHY catalysts / F. Alvarez, F.R. Ribeiro, G. Perot, C. Thomazeau, M. Guisnet // Journal of Catalysis. — 1996. — Vol. 162, No. 2. — P. 179–189. DOI: 10.1006/jcat.1996.0275

24 Choudhury I.R. Pt/H-ZSM-22 hydroisomerization catalysts optimization guided by Single-Event MicroKinetic modeling / I.R. Choudhury, K. Hayasaka, J.W. Thybaut, C.S.L. Narasimhan, J.F. Denayer, J.A. Martens, G.B. Marin // Journal of Catalysis. — 2012. — Vol. 290. — P. 165–176. DOI: 10.1016/j.jcat.2012.03.015

25 Verboekend D. Towards more efficient monodimensional zeolite catalysts: n-alkane hydro-isomerisation on hierarchical ZSM-22 / D. Verboekend, K. Thomas, M. Milina, S. Mitchell, J. Perez-Ramirez, J.P. Gilson // Catalysis Science & Technology. — 2011. — Vol. 1, No. 8. — P. 1331–1335. DOI: 10.1039/c1cy00240f

26 Guczi L. Structure and catalytic properties of iron-containing bimetallic catalysts / L. Guczi // Catalysis Reviews — Science and Engineering. — 1981. — Vol. 23, No. 3. — P. 329–376. DOI: 10.1080/03602458108079640

27 Dezsi I. Characterization of silica supported Pt-Fe catalysts by Mossbauer-spectroscopy / I. Dezsi, D.L. Nagy, M. Eszterle, L. Guczi // Reaction Kinetics and Catalysis Letters. — 1978. — Vol. 8, No. 3. — P. 301–307. DOI: 10.1007/BF02068170

А.К. Жұмабекова, Л.К. Тастанова, Р.О. Орынбасар, Г.Д. Закумбаева

Модификаторлардың Fe-Pt/Al_2O_3 алкандарды гидроөңдеу катализаторларына әсері

Молибден, фосфор және церий қоспаларымен модификацияланған құрамында цеолиті бар Fe-Pt/Al_2O_3 (КТ-17, КТ-18) полифункционалды катализаторлары синтезделді. Модификациялық қоспалардың КТ-17 және КТ-18 каталитикалық қасиеттеріне әсері зерттелді. Әзірленген каталитикалық жүйелер бензин фракциясын алу үшін C_{14} модельдік алканды гидроөңдеу процесінде зерттелген. Реакция өнімдерінде C_4-C_9 изо-алкандар, C_{10}-C_{14} изо-алкандар, C_4-C_{10} алкандар, ароматты көмірсутектер және C_1-C_3 алкандар бар. Қайта өңдеу өнімдеріндегі ауыр көмірсутектердің құрамы 0,2–0,6 %. C_4-C_9 алкандарының 380 °С температурада шығымы 37,9 % құрайды. Физика-химиялық зерттеу әдістерін қолдана отырып, әр түрлі қоспалармен модификацияланған, цеолиткұрамды Fe-Pt/Al_2O_3 катализаторлары күрделі каталитикалық жүйелер болып табылатындығы анықталды. Микродифракция және Мессбауэр спектроскопиясы әдістерімен катализаторлар құрылымындағы Fe-Pt, Fe-Mo, Pt-Mo наноөлшемді гетерокластерлері анықталды. Кластерлердің химиялық құрамына байланысты бөлшектердің мөлшері 20-дан 80 Å-ге дейін өзгереді. КТ-18 катализаторы ауыр алкандарды өңдеу процесінде

жоғары белсенділік танытады. Электронды микроскопия әдісімен катализатордың құрылымы зерттелді, платина (d = 200 Å) және темір (d = 30–50 Å) бөлшектерінің өлшемдері анықталды. КТ-18 каталитикалық жүйесінің белсенділігі КТ-17 катализаторына қарағанда жоғары. КТ катализаторларының басты ерекшелігі — олардың полифункционалдылығы. Алкандарды өңдеу кезінде гидрокрекинг, дегидрогенизация, изомеризация, дегидроциклизация және гидрокүкіртсіздену реакциялары бір уақытта және дәйекті түрде жүреді.

Кілт сөздер: гидроөңдеу, цеолиткұрамды катализаторлар, модификация, полифункционалдық, ауыр алкандар, гидрокрекинг, гидрлеу, нанокластерлер.

А.К. Жумабекова, Л.К. Тастанова, Р.О. Орынбасар, Г.Д. Закумбаева

Влияние модификаторов на Fe-Pt/Al_2O_3 катализаторы гидропереработки алканов

Синтезированы цеолитсодержащие полифункциональные катализаторы Fe-Pt/Al_2O_3 (КТ-17, КТ-18), модифицированные добавками молибдена, фосфора и церия. Исследовано влияние модифицирующих добавок на каталитические свойства КТ-17 и КТ-18. Разработанные каталитические системы изучены в процессе гидропепереработки модельного алкана С14 с получением бензиновой фракции. В продуктах реакции содержатся изо-алканы С4-С9, изо-алканы С10-С14, алканы С4-С10, ароматические углеводороды и алканы С1-С3. Содержание тяжелых углеводородов в продуктах переработки — 0,2–0,6 %. Выход изо-алканов С4-С9 при температуре 380 °С составляет 37,9 %. С помощью физико-химических методов исследования установлено, что модифицированные различными добавками цеолитсодержащие катализаторы Fe-Pt/Al_2O_3 представляют собой сложные каталитические системы. Методами микродифракции и Мессбауэровской спектроскопии в структуре катализаторов обнаружены наноразмерные гетерокластеры Fe-Pt, Fe-Mo, Pt-Mo. В зависимости от химического состава кластеров размер частиц колеблется от 20 до 80 Å. Катализатор КТ-18 проявляет высокую активность в процессе переработки тяжелых алканов. Методом электронной микроскопии исследована структура катализатора, определены размеры частиц платины (d = 200 Å) и железа (d = 30–50 Å). Активность каталитической системы КТ-18 выше, чем у высокодисперсного катализатора КТ-17. Главной особенностью катализаторов КТ является их полифункциональность. При обработке алканов одновременно и последовательно протекают реакции гидрокрекинга, дегидрогенизации, изомеризации, дегидроциклизации и гидрообессеривания.

Ключевые слова: гидропереработка, цеолитсодержащие катализаторы, модификация, полифункциональность, тяжелые алканы, гидрокрекинг, гидрирование, нанокластеры.

References

1 Rana, M.S., Sarmano, V., Ancheyta, J., & Diaz, J. (2007). A review of recent advances on process technologies for upgrading of heavy oils and residua. *Fuel, 86(9)*, 1216–1231. DOI: 10.1016/j.fuel.2006.08.004

2 Okunev, A.G., Parkhomchuk, E.V., Lysikov, A.I., Parunin, P.D., Semeykina, V.S., & Parmon, V.N. (2015). Catalytic hydroprocessing of heavy oil feedstocks. *Russian Chemical Reviews, 84(9)*, 981–999. DOI: 10.1070/RCR4486

3 Sahu, R., Song, B.J., Im, J.S., Jeon, Y-P., & Lee, C.W. (2015). A review of recent advances in catalytic hydrocracking of heavy residues. *Journal of Industrial and Engineering Chemistry, 27*, 12–24. DOI: 10.1016/j.jiec.2015.01.011

4 Fujimoto, K., Chang, J., & Tsubaki, N. (2000). Hydrothermal cracking of residual oil. *Sekiyu Gakkaishi — Journal of the Japan Petroleum Institute, 43(1)*, 25–36.

5 Gillis, D., VanWees, M., Zimmerman, P., & Houde, E. (2010). Upgrading Residues to Maximize Distillate Yields with UOP Uniflex (TM) Process. *Journal of the Japan Petroleum Institute, 53(1)*, 33–41. DOI: 10.1627/jpi.53.33

6 Corma, A., Corresa, E., Mathieu, Y., Sauvanaud, L., Al-Bogami, S., & Al-Ghrami, M. S., et al. (2017). Crude oil to chemicals: light olefins from crude oil. *Catalysis Science & Technology, 7(1),* 12–46. DOI: 10.1039/c6cy01886f

7 Nazarova, G.Y., Ivashkina, E.N., Ivanchina, E.D., Stebeneva, V.I., & Seytenova, G.Z. (2016). Effect of group composition of the vacuum distillate from heavy Kazakhstan and West Siberian oil on the yield of light fractions during the catalytic cracking. *Procedia Engineering, 152*, 18–24. DOI: 10.1016/j.proeng.2016.07.611

8 Kaminski, T., & Husein, M.M. (2018). Thermal cracking of atmospheric residue versus vacuum residue. *Fuel Processing Technology, 181*, 331–339. DOI: 10.1016/j.fuproc.2018.10.014

9 Ghashghaee, M., & Shirvani, S. (2018). Two-Step Thermal Cracking of an Extra-Heavy Fuel Oil: Experimental Evaluation, Characterization, and Kinetics. *Industrial and Engineering Chemistry Research, 57(22),* 7421–7430. DOI: 10.1021/acs.iecr.8b00819

10 Vogt, E.T.C., & Weckhuysen, B.M. (2015). Fluid catalytic cracking: recent developments on the grand old lady of zeolite catalysis. *Chemical Society Reviews, 44(20),* 7342–7370. DOI: 10.1039/c5cs00376h

11 Onoichenko, S.N., Emel'yanov, V.E., & Krylov, I.F. (2003). Current and Promising Automotive Gasolines. *Chemistry and technology of fuels and oils, 39(6)*, 303–308. DOI: 10.1023/B: CAFO.0000011901.59445.22

12 Hajbabaei, M., Karavalakis, G., Miller, J.W., Villela, M., Xu, K.H., & Durbin, T.D. (2013). Impact of olefin content on criteria and toxic emissions from modern gasoline vehicles. *Fuel, 107*, 671–679. DOI: 10.1016/j.fuel.2012.12.031

13 Courty, P., & Gruson, J.F. (2001). Refining Clean Fuels for the Future. *Oil & Gas Science and Technology, 56(5),* 515–524. DOI: 10.2516/ogst:2001041

14 Castaneda, L.C., Munoz, J.A.D., & Ancheyta, J. (2012). Combined process schemes for upgrading of heavy petroleum. *Fuel, 100*, 110–127. DOI: 10.1016/j.fuel.2012.02.022

15 Bellussi, G., Rispoli, G., Landoni, A., Millini, R., Molinari, D., & Montanari, E., et al. (2013). Hydroconversion of heavy residues in slurry reactors: Developments and perspectives. *Journal of Catalysis, 308*, 189–200. DOI: 10.1016/j.jcat.2013.07.002

16 Zaki, T., Mukhtarova, G.S., Al-Sabagh, A.M., Soliman, F.S., Betiha, M.A., & Mahmoud, T., et al. (2018). Slurry-phase catalytic hydrocracking of mazut (heavy residual fuel oil) using Ni-bentonite. *Petroleum Science and Technology, 36(19)*, 1559–1567. DOI: 10.1080/10916466.2018.1490762

17 Martens, J.A., Verboekend, D., Thomas, K., Vanbutsele, G., Perez-Ramirez, J., & Gilson, J.P. (2013). Hydroisomerization and hydrocracking of linear and multibranched long model alkanes on hierarchical Pt/ZSM-22 zeolite. *Catalysis Today, 218*, 135–142. DOI: 10.1016/j.cattod.2013.03.041

18 Batalha, N., Pinard, L., Bouchy, C., Guillon, E., & Guisnet, M. (2013). n-Hexadecane hydroisomerization over Pt-HBEA catalysts. Quantification and effect of the intimacy between metal and protonic sites. *Journal of Catalysis, 307*, 122–131. DOI: 10.1016/j.jcat.2013.07.014

19 Sosnin, G.A., Zaikina, O.O., Eletskii, P.M., & Yakovlev, V.A. (2018). Catalytic steam cracking of vacuum residue in presence of dispersed catalysts based on Mo, Ni, Fe, Co, Al metals. *Bulletin of the Tomsk Polytechnic University — Geo Assets Engineering, 329(12)*, 145–154. DOI: 10.18799/24131830/2018/12/30

20 Mironenko, O.O., Sosnin, G.A., Eletskii, P.M., Gulyaeva, Y.K., Bulavchenko, O.A., & Stonkus, O.A., et al. (2017). Catalytic Steam Cracking of Heavy Crude Oil with Molybdenum and Nickel Nanodispersed Catalysts. *Catalysis in Industry, 9(3)*, 221–229. DOI: 10.1134/S2070050417030084

21 Alphazan, T., Bonduelle-Skrzypczak, A., Legens, C., Gay, A.S., Boudene, Z., & Girleanu, M., et al. (2014). Highly active nonpromoted hydrotreating catalysts through the controlled growth of a supported hexagonal WS2 phase. *ACS Catalysis, 4(12)*, 4320–4331. DOI: 10.1021/cs501311m

22 Funai, S., Fumoto, E., Tago, T., & Masuda, T. (2010). Recovery of useful lighter fuels from petroleum residual oil by oxidative cracking with steam using iron oxide catalyst. *Chemical Engineering Science, 65(1)*, 60–65. DOI: 10.1016/j.ces.2009.03.028

23 Alvarez, F., Ribeiro, F.R., Perot, G., Thomazeau, C., & Guisnet, M. (1996). Hydroisomerization and hydrocracking of alkanes — Influence of the balance between acid and hydrogenating functions on the transformation of n-decane on PtHY catalysts. *Journal of Catalysis, 162(2)*, 179–189. DOI: 10.1006/jcat.1996.0275

24 Choudhury, I.R., Hayasaka, K., Thybaut, J.W., Narasimhan, C.S.L., Denayer, J.F., & Martens, J.A., et al. (2012). Pt/H-ZSM-22 hydroisomerization catalysts optimization guided by Single-Event MicroKinetic modeling. *Journal of Catalysis, 290*, 165–176. DOI: 10.1016/j.jcat.2012.03.015

25 Verboekend, D., Thomas, K., Milina, M., Mitchell, S., Perez-Ramirez, J. & Gilson, J.P. (2011). Towards more efficient monodimensional zeolite catalysts: n-alkane hydro-isomerisation on hierarchical ZSM-22. *Catalysis Science & Technology, 1(8)*, 1331–1335. DOI: 10.1039/c1cy00240f

26 Guczi, L. (1981). Structure and catalytic properties of iron-containing bimetallic catalysts. *Catalysis Reviews — Science and Engineering, 23(3)*, 329–376. DOI: 10.1080/03602458108079640

27 Dezsi, I., Nagy, D.L., Eszterle, M., & Guczi, L. (1978). Characterization of silica supported Pt-Fe catalysts by Mossbauer-spectroscopy. *Reaction Kinetics and Catalysis Letters, 8(3)*, 301–307. DOI: 10.1007/BF02068170

Information about authors

Zhumabekova, Arai Kerimakynovna — Candidate of chemical sciences, Associate Professor, Manash Kozybayev North Kazakhstan State University, Petropavlovsk, Pushkin str., 86, 150000, Kazakhstan; e-mail: zhumabekova_ak@mail.ru; https://orcid.org/0000–0001–6743–8953.

Tastanova, Lyazzat Knashevna — Candidate of chemical sciences, Associate Professor, K. Zhubanov Aktobe Regional University, Aktobe, A. Moldagulova ave., 34, 030000, Kazakhstan; e-mail: lyazzatt@mail.ru; https://orcid.org/0000–0002–9236–5909;

Orynbassar, Raigul Orynbassarovna — Candidate of chemical sciences, Associate Professor, Al-Farabi Kazakh National University, Almaty, al-Farabi Ave., 71, 050040, Kazakhstan; e-mail: raihan_06_79@mail.ru; https://orcid.org/0000–0002–6198–3018.

Zakumbaeva, Gaukhar Daulenovna — Senior researcher, D.V. Sokolskii Institute of Fuel, Catalysis and Electrochemistry, Almaty, Kunayev Str., 142, 050010, Kazakhstan; e-mail: orynbassar.raigul@gmail.com.